

# Square Openings as Sources of Stress Concentration in Parts of Machines and Devices

Mladen RADOJKOVIĆ\*, Blaža STOJANOVIĆ, Saša MILOJEVIĆ, Dejan MARIĆ\*, Slobodan SAVIĆ, Aleksandar SKULIĆ, Božidar KRSTIĆ

**Abstract:** In this paper the impact of square opening, as a source of stress concentration, on the distribution of stress in parts of machines and devices is considered. The fact is that these forms of the openings occur less in practice, but the knowledge of the influence of the square opening on the stress distribution, from the aspect of its size, the radius of the angles curvature and positions in relation to the attack lines of the external load, is very important for those who are dealing with designing and constructing parts that contain such shapes of openings. Therefore, the aim of this paper is to analyse the influence of the position and radius of the angles curvature of the square opening on the stress distribution in parts of machines and devices, made of isotropic materials, because these materials are most often used and common in engineering practice. In order to obtain the results of the stress distribution, analytical and numerical methods were used in this paper.

**Keywords:** curvature radius; machines and devices; square opening; stress concentration; stress distribution

## 1 INTRODUCTION

The machine part is the basic part of a machine or device that performs a specific function. Mechanical parts are more commonly connected by making mechanical subassemblies, machine assemblies and machine groups. By connecting machine parts, machine subassemblies, machine assemblies and machine groups into one functional whole, machines and devices, or wider machine systems, are created. In order for machines and devices to perform their function, all their components must perform their individual functions. On the functions performed by these components depend their dimensions, shape and geometry.

Machine parts that are part of machines and devices can be of different dimensions and geometric shapes, and often contain openings, holes, grooves, notches and other geometric discontinuities. These discontinuities are designed to create an interconnection of elements (e.g. by screws, rivets), weight reduction, lubrication and other reasons. However, the existence of such discontinuities in machine parts generally adversely affects the size and distribution of stress in these parts. In order to reliably construct parts and even the entire structure, it is necessary to know the stress distribution, especially in the geometric discontinuity zones, because the tests have shown that the highest values of the stress occur in those areas. And it is precisely the high values of the stress at these areas that cause the breakdown of parts, and even the devastation of the entire structures. In order to prevent such phenomena, a good knowledge of this problem is necessary, i.e. the problem of stress distribution and concentration.

The most common forms of discontinuity in parts of machines and devices are the openings. They are sources of stress concentration, i.e. places where the stresses increase rapidly. Therefore, the problem of stress distribution and concentration in parts of machines and devices should be taken seriously, and this problem should be addressed with a lot of responsibility. In studying such problems, the basic and most important task is to properly examine all the parameters that affect the stress state.

In addition to experimental methods, which provide the ability to obtain reliable data on the stress state in the analysis of parts and the entire construction, for a more

detailed calculation of the stress state analytical and numerical methods can also be used, taking into account other factors that influence the stress state. Solving tasks using analytical methods is usually reduced to solving differential equations, ordinary or partial, with meeting the appropriate boundary conditions [1-3]. In numerical methods, the fundamental equations of the Theory of elasticity describing the state of stress [4, 5] are solved by the approximate numerical method [6-8].

A large number of researchers have contributed to the study of the distribution and concentration of stress in parts of weakened openings of different shapes, made of both isotropic and anisotropic materials [9-19]. Silpa et al. [20] carried out a structural analysis of thin isotropic and orthotropic plates with a circular opening using the finite element method and Rahman [21] studies the stress distribution in uniaxial stressed steel plates of the finite dimensions weakened by rectangular aperture using the finite element method. Jafari [22] gives the distribution of stress and displacement around a rectangular hole in an orthotropic infinite plate exposed to heat flux at infinity, as well as the influence of the position of the hole, the angle of the orthotropic plate fibres, the angle of heat flux and the aspect ratio. Hussein et al. [23] investigate the failure behaviour of a composite plate under the influence of various factors such as fibre content, load angle, hole dimension ratio and fibre orientation in the composite plate. Using ANSYS software Konieczny et al. [24] analyse isotropic axisymmetric circular plates of finite dimensions, loaded with concentric forces of different values in the geometric centre of the plate, where the plates have holes arranged at ten different distances. In their paper, Patel and Desai [25] study the stress concentration around an elliptical hole in a large rectangular plate subjected to linearly varying in-plane loading on two opposite edges and Zappalorto [26] gives universal equations for stress distribution in orthotropic plates finite sizes with blunt notches and holes. Meštrović [27] gives the basic equations that represent the relationship between the displacement vector and the strain vector, as well as between the components of the stress tensor and the components of the strain tensor. Kalay et al. [28] are dealing with comparative 3D computer finite element study of stress distribution and stress transfer in small

diameter conical dental implants. Tuna and Trovalusci [28] analyze the stress distribution around an elliptical hole in a plate with "implicit" and "explicit" non-local models. In their paper, Turnić et al. [30] consider the stress analysis of steel I girders subjected to patch loading for different lengths of load. In doing so, they analyse the values of stresses obtained experimentally with the results obtained in the ANSYS software.

In this paper, software ANSYS 5.4 [31] was used to obtain the results on stress distribution, and the obtained results were compared with the results obtained analytically.

## 2 REVIEW OF EQUATIONS AND RESULTS OF STRESS DISTRIBUTION OBTAINED BY ANALYTICAL METHODS

Analytical methods determine the mathematical functions that define a solution in a closed form, and they are based on the laws of Resistance of Materials and Theory of Elasticity [4, 5]. To obtain the result of the stress distribution, i.e. the stress values in the points of the contour of the opening, of the analytical methods, in this paper the method of complex variable was used. The essence of this method consists in the fact that the stress function is expressed by the analytic functions of a complex variable, and the stress components using a certain stress function of a complex variable, with the satisfaction of certain boundary or contour conditions. The analytic functions of complex variables are represented in the form of order degrees with complex constant coefficients, and when solving specific problems, the orders with the finite number of members are used.

For an irregular square opening shown in Fig. 1, according to [2, 3], when in the equation for the mapping function  $z = \omega(\zeta)$  two members are retained, the equation gets the following form:

$$z = x + iy = \omega(\zeta) = R \left( \frac{1}{\zeta} - \frac{1}{6} \zeta^3 \right) \quad (1)$$

where  $\zeta$  is an independent variable.

When in Eq. (1)  $\zeta = \rho e^{i\theta} = \rho(\cos\theta + i \sin\theta)$  and  $\rho = 1$  is put, and then real and imaginary parts are separated, the parametric equations of the contour of the opening are obtained in the following form:

$$\begin{aligned} x &= R \left( \cos\theta - \frac{1}{6} \cos 3\theta \right) \\ y &= -R \left( \sin\theta + \frac{1}{6} \sin 3\theta \right) \end{aligned} \quad (2)$$

where:  $\rho$  is the constant,  $\theta$  the angle between the normal at the point on the contour of the opening and the  $x$  axis and is measured in the circumference of the contour in the positive mathematical direction,  $R$  the length of the side of the regular square opening.

According to [2, 3], the relationship between the length of the side of the regular square opening  $R$  and the length of the side of the irregular square opening  $a$  (Fig. 1) is:

$$R = \frac{3}{5}a \quad (3)$$

and the radius of curvature of the angles of the irregular square opening:

$$r_{\theta=45^\circ} = \frac{1}{10}R = \frac{3}{50}a = 0.06a \quad (4)$$

The stress functions  $\varphi(\zeta)$  and  $\psi(\zeta)$  for this case, according to [2, 3], have the following form:

$$\begin{aligned} \varphi(\zeta) &= pR \left[ \frac{1}{4\zeta} + \left( \frac{3}{7} \cos 2\alpha + i \frac{3}{5} \sin 2\alpha \right) \zeta + \frac{1}{24} \zeta^3 \right], \\ \psi(\zeta) &= -pR \left[ \frac{e^{-2i\alpha}}{2\zeta} + \right. \\ &\quad \left. + \frac{13\zeta - 26 \left( \frac{3}{7} \cos 2\alpha + i \frac{3}{5} \sin 2\alpha \right) \zeta^3}{12(2 + \zeta^4)} \zeta^3 \right] \end{aligned} \quad (5)$$

The stress Eq. (5) in the case when the attack lines of the external tensile surface forces  $p$  are parallel to the  $x$  axis ( $\alpha = 0$ ), i.e. under the condition  $\sigma_x^{(\infty)} = p$ , and  $\sigma_y^{(\infty)} = \tau_{xy}^{(\infty)} = 0$ , will have the form:

$$\begin{aligned} \varphi(\zeta) &= pR \left[ \frac{1}{4\zeta} + \frac{3}{7} \zeta + \frac{1}{24} \zeta^3 \right], \\ \psi(\zeta) &= -pR \left[ \frac{1}{2\zeta} + \frac{91\zeta - 78\zeta^3}{84(\zeta^4 + 2)} \right] \end{aligned} \quad (6)$$

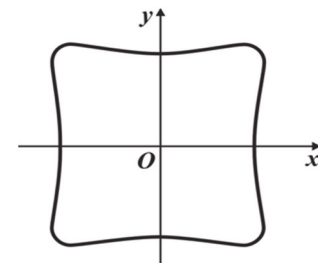


Figure 1 An irregular square opening of the radius of the angle curvature of  $r = 0.06a$

By substituting the corresponding values of the functions  $\omega(\zeta)$  Eq. (1) and  $\varphi(\zeta)$  Eq. (6) into the equation:

$$\sigma_\theta = 4Re \left[ \frac{\varphi'(\sigma)}{\omega'(\sigma)} \right] \quad (7)$$

assuming that  $\zeta = \rho e^{i\theta} = \rho(\cos\theta + i \sin\theta)$  and  $\rho = 1$ , a formula is obtained for determining the stress on the contour of the irregular square opening shown in Fig. 1, in the following form:

$$\sigma_\theta = \frac{8p}{5 + 4\cos 4\theta} \left( \frac{3}{8} - \frac{9}{7} \cos 2\theta \right) \quad (8)$$

By changing the values for  $\theta$  from  $0^\circ$  to  $360^\circ$  in Eq. (8), the stress values at the contour points of the given opening are obtained, but due to the complete symmetry, in this case it is possible to limit it to the interval  $0^\circ$  to  $90^\circ$ .

At  $\alpha = \pi/4$ , i.e. in the case where the angle between the attacking lines of the external tensile surface forces and the  $x$  axis is  $45^\circ$ , according to [2, 3], the stress functions have the following form:

$$\varphi(\zeta) = pR \left[ \frac{1}{4\zeta} + i \frac{3}{5}\zeta + \frac{1}{24}\zeta^3 \right], \quad (9)$$

$$\psi(\zeta) = pR \left[ \frac{i}{2\zeta} + \frac{65\zeta - i78\zeta^3}{60(2+\zeta^4)} \right]$$

and the stresses in the points of the opening contour:

$$\sigma_\theta = \frac{8p}{5+4\cos4\theta} \left( \frac{3}{8} - \frac{3}{5}\sin2\theta \right) \quad (10)$$

For an arbitrary value of the angle  $\alpha$ , the stress values  $\sigma_\theta$  at the contour of the irregular square opening shown in Fig. 1, according to [2, 3], are obtained by the equation:

$$\sigma_\theta = \frac{8p}{5+4\cos4\theta} \left( \frac{3}{8} - \frac{9}{7}\cos2\alpha\cos2\theta - \frac{3}{5}\sin2\alpha\sin2\theta \right) \quad (11)$$

For an irregular square opening shown in Fig. 2, according to [2, 3], when in the equation for the mapping function  $\omega(\zeta)$  two members are retained, the equation gets the following form:

$$\omega(\zeta) = R \left( \frac{1}{\zeta} - \frac{1}{6}\zeta^3 + \frac{1}{56}\zeta^7 \right) \quad (12)$$

By increasing the number of members in the expression for the mapping function  $\omega(\zeta)$ , the radius of curvature of the angles of an irregular square opening decreases, and the deviation of the sides from the straight lines is less. The radius of the curvature of the opening angles in this case will be  $r_{\theta=45^\circ} = 0.0245a$ .

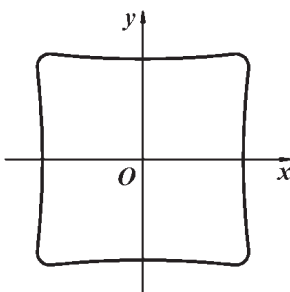


Figure 2 An irregular square opening of the radius of the angle curvature of  $r = 0.0245a$

The stress functions  $\varphi(\zeta)$  and  $\psi(\zeta)$  for this case, according to [2, 3], have the following form:

$$\begin{aligned} \varphi(\zeta) = pR & \left[ \frac{0.25}{\zeta} + (0.426\cos2\alpha + \right. \\ & + i0.608\sin2\alpha)\zeta + 0.46\zeta^3 + (0.008\cos2\alpha - \right. \\ & - i0.011\sin2\alpha)\zeta^5 - 0.004\zeta^7 \Big] + 0.046\zeta^3 + \\ & + (0.008\cos2\alpha - i0.011\sin2\alpha)\zeta^5 - 0.004\zeta^7 \Big] - \\ & - \frac{0.026\zeta^5 + (0.29\cos2\alpha - i0.68\sin2\alpha)\zeta^7}{1 + 0.5\zeta^4 - 0.125\zeta^8} \end{aligned} \quad (13)$$

At  $\alpha = 0$ , the stress functions  $\varphi(\zeta)$  and  $\psi(\zeta)$  Eq. (14), according to [2, 3], will have the following form:

$$\begin{aligned} \varphi(\zeta) = pR & \left[ \frac{0.25}{\zeta} + 0.426\zeta + 0.046\zeta^3 + 0.008\zeta^5 - 0.004\zeta^7 \right], \\ \psi(\zeta) = -pR & \left[ \frac{0.5}{\zeta} + \right. \\ & + \frac{0.548\zeta - 0.457\zeta^3 - 0.026\zeta^5 - 0.029\zeta^7}{1 + 0.5\zeta^4 - 0.125\zeta^8} \end{aligned} \quad (14)$$

and at  $\alpha = \pi/4$ :

$$\begin{aligned} \varphi(\zeta) = pR & \left[ \frac{0.25}{\zeta} + i0.608\zeta + 0.046\zeta^3 - \right. \\ & - i0.011\zeta^5 - 0.004\zeta^7 \Big], \\ \psi(\zeta) = pR & \left[ \frac{0.5i}{\zeta} - \right. \\ & - \frac{0.548\zeta - i0.672\zeta^3 - 0.026\zeta^5 + i0.068\zeta^7}{1 + 0.5\zeta^4 - 0.125\zeta^8} \end{aligned} \quad (15)$$

To evaluate the influence of the radius of the angles curvature of the square opening on the stress distribution on the contour of the opening, in Tab. 1 the stress values  $\sigma_\theta$  are given [2, 3].

For an irregular square opening shown in Fig. 3, according to [2, 3], when in the equation for the mapping function  $\omega(\zeta)$  four members are retained, the equation gets the following form:

$$\omega(\zeta) = R \left( \frac{1}{\zeta} - \frac{1}{6}\zeta^3 + \frac{1}{56}\zeta^7 + \frac{1}{176}\zeta^{11} \right) \quad (16)$$

and the radius of curvature of the angles of the irregular square opening (Fig. 3) will be  $r = 0.014a$ .

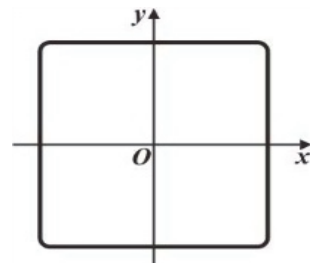


Figure 3 An irregular square opening of the radius of the angle curvature of  $r = 0.014a$

According to [2, 3], the stress functions  $\varphi(\zeta)$  and  $\psi(\zeta)$  at  $\alpha = \pi/2$ , i.e. for  $\sigma_x^{(\infty)} = 0$ , and  $\sigma_y^{(\infty)} = p$ ,  $\tau_{xy}^{(\infty)} = 0$ , will have the form of:

$$\begin{aligned}\varphi(\zeta) &= pR \left[ \frac{0.25}{\zeta} - 0.425\zeta + 0.0476\zeta^3 - \right. \\ &\quad \left. - 0.0086\zeta^5 - 0.0060\zeta^7 + 0.0024\zeta^9 + 0.0014\zeta^{11} \right] \\ \psi(\zeta) &= -pR \left[ \frac{0.5}{\zeta} - \right. \\ &\quad \left. - \frac{0.479\zeta - 0.457\zeta^3 + 0.269\zeta^5 - 0.037\zeta^7}{1 + 0.5\zeta^4 - 0.125\zeta^8 + 0.063\zeta^{12}} - \right. \\ &\quad \left. - \frac{0.073\zeta^9 - 0.017\zeta^{11} - 0.031\zeta^{13}}{1 + 0.5\zeta^4 - 0.124\zeta^8 + 0.063\zeta^{12}} \right]\end{aligned}\quad (17)$$

**Table 1** The values  $\sigma_\theta$  at the contour of the square opening

	$\sigma_\theta / \text{N/m}^2$			
$\theta / {}^\circ$	$\alpha = 0, r = 0.06a$	$\alpha = 0, r = 0.0245a$	$\alpha = \pi/4, r = 0.06a$	$\alpha = \pi/4, r = 0.0245a$
0	-0.808	-0.936	0.333	0.412
35	-0.268	-0.544	3.880	6.564
40	0.980	0.605	6.223	9.672
45	3.000	4.368	7.800	1.516
50	3.860	4.460	6.223	9.672
55	3.366	2.888	3.880	6.564
90	1.472	1.760	0.333	0.412

The stress values  $\sigma_\theta$  on the contour of the opening at  $\alpha = \pi/2$ , according to [2, 3], are given in Tab. 2.

**Table 2** The values  $\sigma_\theta$  at the contour of the square opening

$\theta / {}^\circ$	$\sigma_\theta / \text{N/m}^2$	$\theta / {}^\circ$	$\sigma_\theta / \text{N/m}^2$
0	1.616	50	0.265
15	1.802	60	-0.702
30	1.932	75	-0.901
40	4.230	90	-0.871
45	5.763	-	-

### 3 REVIEW OF THE RESULTS OF THE STRESS DISTRIBUTION OBTAINED BY NUMERICAL METHOD

It is known that numerical methods can be successfully used to obtain the results of the stress distribution in parts of machines and devices that are weakened by the openings. Considering the nature of the problem considered in this paper, the method of finite elements is used. As the method requires the use of computers and the corresponding software packages, the ANSYS 5.4 software package [30] is used to obtain the results of the stress distribution in this paper. As with other software packages, certain operations are automated, which allows the automatic generation of the finite elements network.

Using the method of finite elements, and in accordance with the methodology set out in [3, 6, 7], in this paper, the results of the stress distribution  $\sigma_{\max}$  were obtained. The results that have been reached relate to the elements of a plate type, dimensions in all cases  $5 \text{ m} \times 2 \text{ m} \times 0.1 \text{ m}$ . They are weakened by the square opening of the side  $a = 100 \text{ mm}$ , and the axes of symmetry coincide with the  $x$  axis and  $y$  axis directions. The load is uniaxial, and the intensity of the tensile surface forces is, in all examples,  $p = 1 \text{ N/m}^2$ , whereat in all the examples  $\alpha$  is the angle

between the attack lines of the external tensile surface forces and the  $x$  axis. The material from which the plates are made is steel, with a modulus of elasticity  $E = 2.1 \times 10^5 \text{ MPa}$  and Poisson's coefficient  $\mu = 0.33$ . In the examples, 2D triangular solid finite elements were used.

Standard triangular finite element for planar constructions loaded in their plane is a triangular finite element with 6 degrees of freedom. The vertices of the triangle are also the nodes, and the degrees of freedom are unknown displacements in two coordinate directions in the vertices of the triangle, the nodes of the linear triangular finite element (eng. three-noded linear triangular element). The advantage of this finite element is distinct simplicity that enables the implementation of the element in various types of two-dimensional edge tasks. The limited accuracy of the solutions obtained using this element results from the linear approximation of the field displacement, which implies constant deformation and constant stress on the element. In the areas for larger increments of displacement, it is necessary to thicken the mesh of finite elements, which is actually practical and is not a significant problem. The linear triangular finite element is ideal for display due to its simplicity application of the finite element method (FEM) to two-dimensional boundary problems. The basic equations that give the connection between the displacement vector and the strain vector, as well as between the components of the stress tensor and the components of the strain tensor can be found in [7, 27].

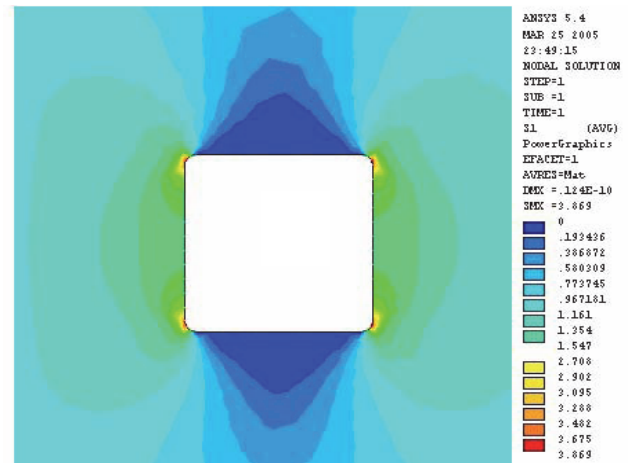


**Figure 4** The stress distribution  $\sigma_{\max}$  in the plate weakened by the square opening of the side  $a = 100 \text{ mm}$ , of the radius of the curvature of the opening angle  $r = 6 \text{ mm}$  at  $\alpha = 0^\circ$

In Fig. 4 and Fig. 5 the distribution of the maximum normal tensile stress  $\sigma_{\max}$  is shown in a flat isotropic plate weakened by a square opening in the middle of the plate. In the example of Fig. 4 the square opening in the plate is made so that the sides are parallel to the sides of the plate, the tension is done along the length of the plate side at  $\alpha = 0$ . In the example of Fig. 5 the square opening in the plate is made so that the sides are diagonal to the sides of the plate, the tension is done along the length of the plate side at  $\alpha = \pi/4$ . The radius of curvature of the angles of the square opening in both cases is  $r = 6 \text{ mm}$ . From Fig. 4 and Fig. 5 we see that the highest values of this stress  $\sigma_{\max}$  occur at the points of the contour of the opening, near the angles of the square opening (the red area of the stress field in Fig.

4 and Fig. 5). The highest stress value for the case in Fig. 4 is  $\sigma_{\max} = 3.869 \text{ N/m}^2$ , and in the case in Fig. 5 it is  $\sigma_{\max} = 7.317 \text{ N/m}^2$ .

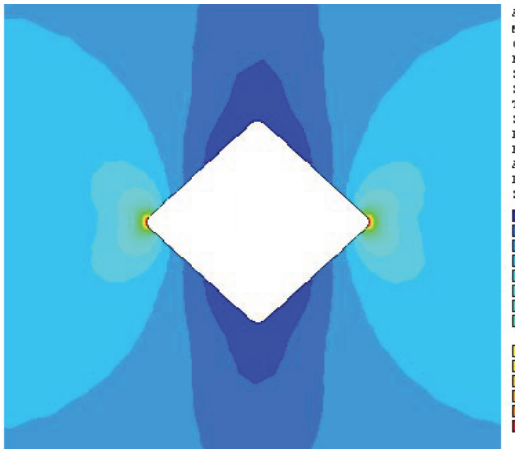


Figure 5 The stress distribution  $\sigma_{\max}$  in the plate weakened by the square opening of the side  $a = 100 \text{ mm}$ , the radius of the curvature of the opening angle  $r = 6 \text{ mm}$  at  $\alpha = \pi/4$

Fig. 6 shows the distribution of the maximum normal tensile stress  $\sigma_{\max}$  in the case when  $r = 2.45 \text{ mm}$ , under the same conditions as in Fig. 4, and Fig. 7 shows the distribution of the same stress at  $r = 2.45 \text{ mm}$  and the same conditions as in Fig. 5. From Fig. 4 and Fig. 5 it can be seen that the highest values of this stress are obtained at the points of the contour of the opening, near the angles of the square opening (the red area of the stress field in Fig. 6 and Fig. 7). The highest stress value for the case in Fig. 6 is  $\sigma_{\max} = 5.13 \text{ N/m}^2$ , and in the case in Fig. 7 it is  $\sigma_{\max} = 10.441 \text{ N/m}^2$ .

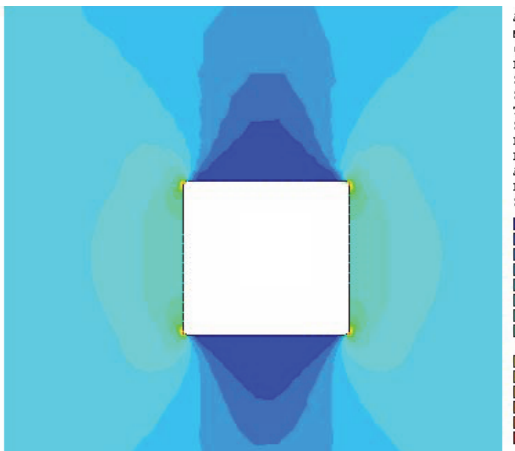


Figure 6 The stress distribution  $\sigma_{\max}$  in the plate weakened by the square opening of the side  $a = 100 \text{ mm}$ , the radius of the curvature of the opening angle  $r = 2.45 \text{ mm}$  at  $\alpha = 0^\circ$

Fig. 8 shows the distribution of the maximum normal tensile stress  $\sigma_{\max}$  in the case when the square opening in the plate is made so that its sides are parallel to the sides of the plate, the tension is done along the shorter side of the panel at  $= \alpha \pi/2$ . The radius of curvature of the angles of the square opening is  $r = 1.4 \text{ mm}$ . The highest values of this stress, in this case as well, are obtained at the points of the contour of the opening near the angles of the square opening (red area of the stress field in Fig. 8). The highest stress value for the case in Fig. 8 is  $\sigma_{\max} = 6.396 \text{ N/m}^2$ .

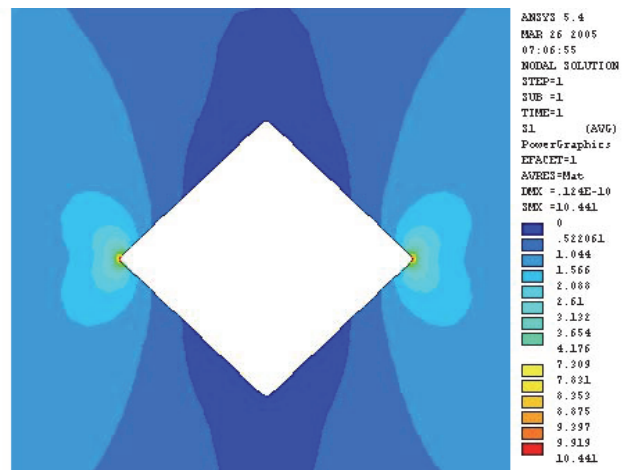


Figure 7 The stress distribution  $\sigma_{\max}$  in the plate weakened by the square opening of the side  $a = 100 \text{ mm}$ , the radius of the curvature of the opening angle  $r = 2.45 \text{ mm}$  at  $\alpha = \pi/4$

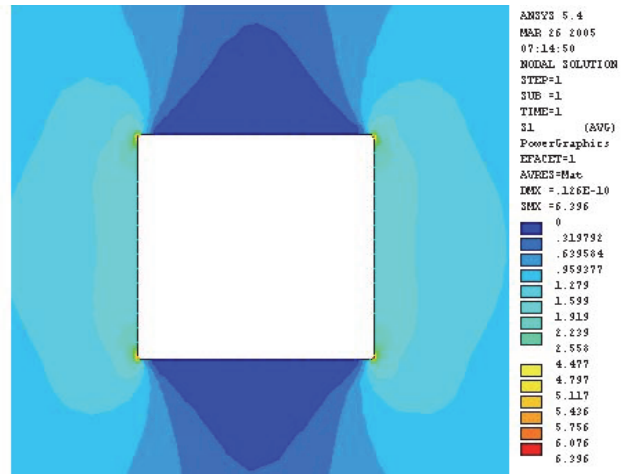


Figure 8 The stress distribution  $\sigma_{\max}$  in the plate weakened by the square opening of the side  $a = 100 \text{ mm}$ , the radius of the curvature of the opening angle  $r = 1.4 \text{ mm}$  at  $\alpha = \pi/2$

#### 4 COMPARISON OF THE RESULTS OBTAINED ANALYTICALLY AND NUMERICALLY

In order to determine the reliability of the results obtained numerically, by FEM, a comparison with the results obtained by analytical method was made using the complex variable method [2, 3]. The obtained values of the maximum normal tensile stress  $\sigma_{\max}$  for the uniaxial tensed homogeneous isotropic plate, impaired by the square opening of the length of the side  $a = 100 \text{ mm}$ , at different values of the radius of the curvature of the angles of the square opening ( $r = 6 \text{ mm}$ ,  $r = 2.45 \text{ mm}$  and  $r = 1.4 \text{ mm}$ ) and at different angles between the attack lines of the external tensile surface forces and the direction of the  $x$  axis ( $\alpha = 0$ ,  $\alpha = \pi/4$ ,  $\alpha = \pi/2$ ).

Tab. 3 shows the highest values of the maximum normal tensile stress  $\sigma_{\max}$  obtained analytically by the complex variable method (ANAL) and numerically by the (FEM).

Table 3 The stress values  $\sigma_{\max}$

Metoda	$\sigma_{\max} / \text{N/m}^2$				
	$r = 6 \text{ mm}$		$r = 2.45 \text{ mm}$		$r = 1.4 \text{ mm}$
	$\alpha = 0$	$\alpha = \pi/4$	$\alpha = 0$	$\alpha = \pi/4$	$\alpha = \pi/2$
ANAL	3.860	7.800	4.460	11.516	5.763
FEM	3.869	7.317	5.130	10.441	6.396

By analyzing the results from Tab. 3, obtained analytically by the method of complex variable and numerically using the FEM, it can be concluded that the highest values of the voltage are obtained at the points of the contour of the square opening. Based on the results in Tab. 3, it can be seen that the maximum values of the normal tensile stress  $\sigma_{\max}$  in parts of the type of plates, weakened by the square opening in the middle and loaded with external tensile surface forces, occur at the points of the opening contour near the angles of the square opening, and by decreasing the radius of the curvature of the angles of the square opening the stresses are obtained at these points and vice versa. On the basis of the obtained results, it can be concluded that the position of this shape of the opening has a major influence on the stress distribution, and that as the most unfavorable is the case when the attack lines of the external tensile surface forces close the angle of  $45^\circ$  with the direction  $x$  axis (Fig. 5 and Fig. 7).

## 5 CONCLUSION

In order to obtain the results of the stress distribution, analytical and numerical methods were used in this paper. From the analytical methods the method of complex variables was used, since it showed exceptional results in the study of stress distribution and concentration, and from the numerical method the FEM was used, as one of the most widely used methods.

In this paper, the results are obtained on the distribution of the maximum normal tensile stress in the elements of plate type, uniaxial tensed by the external surface forces. The plates are weakened in the middle by the square shaped opening with different values of the radius of the curvature, because in practice there are no tools for making such openings whose curvature radii are equal to zero, and if there were such tools, the production of openings in parts would not be possible, because cracks and splits would appear during the course of their production, making the made parts unusable. Therefore, this paper considers the influence of the curvature radius of the square opening on the stress distribution. It started with higher radius values, and then decreasing the values. The tests have shown that the highest values of the stress were obtained precisely at these points and that the stresses increase with decreasing radius of the curvature of the angles of the square opening.

Further, in order to create a complete picture of the effect of a square opening on the stress distribution, it is also necessary to know the influence of the position of the opening on the stress state. For the purpose, the plates weakened by a square opening were examined, so that in one case the sides were parallel to the sides of the plate, and in the second case diagonal. The tests have shown that the position of the opening in the second case is much more unfavorable in terms of stress concentration, because at the points of the contours located in the angles of the square opening there are significantly higher stress values.

Finally, it should be emphasized that, although these forms of the openings are less likely to occur in practice, consideration and study of their influence on the distribution and concentration of stress is of great importance for the theory. Such tests have shown that the influence of both the radius of the curvature of the angles

of the square opening and of the opening position is great and that it must be taken into account when they are encountered in practice.

Certainly, these tests can be of great benefit to researchers in this field in order to compare the obtained values and make certain conclusions and statements, as well as to the engineers when designing and constructing parts that contain such forms of the opening.

## 6 REFERENCES

- [1] Muskhelishvili, N. I. (1966). *Some fundamental problems of the mathematical theory of elasticity*. Moscow, Nauka.
- [2] Savin, G. N. (1968). *Stress distribution around holes*. Kiev, Naukova Dumka.
- [3] Radojković, M. (2005). *Stress distribution in the planar isotropic field weakened by holes*. Kragujevac, Faculty of Mechanical Engineering.
- [4] Timoshenko, S. P. & Goodier, J. N. (1987). *Theory of elasticity*. New York, McGraw-Hill.
- [5] Rašković, D. (1985). *Theory of elasticity*. Belgrade, Scientific book.
- [6] Bathe, K. J. & Wilson, E. L. (1976). *Numerical methods in finite element analysis*. New Jersey, Prentice-Hall, Englewood Cliffs.
- [7] Nikolić, V. (1999). *Mechanical analysis of gears*. Monograph. Kragujevac, Cipmes, Faculty of Mechanical Engineering.
- [8] Kojić, M., Slavković, R., Živković, M., & Grujović, N. (1998). *Finite element method I-linear analysis*. Kragujevac, Faculty of Mechanical Engineering.
- [9] Hwai-Chung, W. & Bin, M. (2003). On stress concentrations for isotropic/orthotropic plates and cylinders with a circular hole. *Composites Part B: Engineering*, 34(2), 127-134. [https://doi.org/10.1016/s1359-8368\(02\)00097-5](https://doi.org/10.1016/s1359-8368(02)00097-5)
- [10] Zakora, S. V., Chekhov, V. N., & Shnerenko, K. I. (2004). Stress concentration around a circular hole in a transversely isotropic spherical shell. *International Applied Mechanics*, 40(12), 1391-1397. <https://doi.org/10.1007/s10778-005-0045-0>
- [11] Shaldyrvan, V. A. (2007). Some results and problems in the three-dimensional theory of plates. *International Applied Mechanics*, 43(2), 160-181. <https://doi.org/10.1007/s10778-007-0014-x>
- [12] Kondratenko, O. A. (2008). Stress state around a circular hole in a prestressed transversely isotropic spherical shell. *International Applied Mechanics*, 44(2), 167-173. <https://doi.org/10.1007/s10778-008-0035-0>
- [13] Jain, N. K. & Mittal, N. D. (2008). Finite element analysis for stress concentration and deflection in isotropic, orthotropic and laminated composite plates with central circular hole under transverse static loading. *Materials Science and Engineering: A*, 498(1-2), 115-124. <https://doi.org/10.1016/j.msea.2008.04.078>
- [14] Vanam, B. C. L., Rajyalakshmi, M., & Inala, R. (2012). Static analysis of an isotropic rectangular plate using finite element analysis (FEA). *Journal of Mechanical Engineering Research*, 4(4), 148-162. <https://doi.org/10.5897/jmer11.088>
- [15] Khoma, I. Y. & Starygina, O. A. (2012). Influence of elastic properties on the stress state of a nonthin transversely isotropic plate with a circular hole. *International Applied Mechanics*, 48(1), 67-79. <https://doi.org/10.1007/s10778-012-0506-1>
- [16] Mallikarjun, B., Dinesh, P., & Paashivamurthy, K. I. (2012). Finite element analysis of elastic stresses around holes in plate subjected to uniform tensile loading. *Bonefring International Journal of Industrial Engineering and Management Science*, 2(4), 136-142. <https://doi.org/10.9756/BIJEMS.1824>

- [17] Banerjee, M., Jain, N. K., & Sanyal, S. (2013). Stress Concentration in Isotropic & Orthotropic Composite Plates with Centre Circular Hole Subjected to Transverse Static Loading. *International Journal of Mechanical and Industrial Engineering (IJMIE)*, 3(1), 109-113.
- [18] Nikolić, V., Doličanin, Č., Radojković, M., & Doličanin, E. (2015). Stress distribution in an anisotropy plane field weakened by an elliptical hole. *Tehnički vjesnik-Technical Gazette*, 22(2), 329-335. <https://doi.org/10.17559/tv-20131102132713>
- [19] Ćirković, B., Čamagić, I., Vasić, N., Burzić, Z., & Folić, B. (2015). Analysis of the supporting structure of composite material tool machine using the finite element method. *Technical Gazette*, 22(1), 95-98. <https://doi.org/10.17559/TV-20130928105016>
- [20] Silpa, V. J. K., Raghu Vamsi, B. V. S., & Gowtham Kumar, K. (2017). Structural Analysis of thin isotropic and orthotropic plates using finite element analysis. *SSRG International Journal of Mechanical Engineering (SSRG-IJME)*, 4(6), 13-24. <https://doi.org/10.14445/23488360/ijme-v4i6p104>
- [21] Rahman, S. (2018). Stress Analysis of Finite Steel Plate with a Rectangular Hole Subjected to Uniaxial Stress Using Finite Element Method. *Journal of Marine Science: Research & Development*, 8(3), 1-6. <https://doi.org/10.4172/2155-9910.1000254>
- [22] Jafari, M. (2019). Thermal stress analysis of orthotropic plate containing a rectangular hole using complex variable method. *European Journal of Mechanics-A/Solids*, 73, 212-223. <https://doi.org/10.1016/j.euromechsol.2018.08.001>
- [23] Hussein, E. Q., Sadeq, B. R., & Rashid, F. L. (2020). Failure Analysis of Composites Plate with Central Opening Hole Subject to Arbitrary Tension Load. *Journal of Mechanical Engineering Research and Developments*, 43(1), 36-47.
- [24] Konieczny, M. M., Achtelik, H., & Gasiak, G. (2020). Finite Element Analysis (FEA) and experimental stress analysis in circular perforated plates loaded with concentrated force. *Frattura ed Integrità Strutturale*, 51, 164-173. <https://doi.org/10.3221/IGF-ESIS.51.13>
- [25] Patel, A. & Desai, C. K. (2020). Stress concentration around an elliptical hole in a large rectangular plate subjected to linearly varying in-plane loading on two opposite edges. *Theoretical and Applied Fracture Mechanics*, 106, 102432. <https://doi.org/10.1016/j.tafmec.2019.102432>
- [26] Zappalorto, M. (2020). Universal equations for the mode I stress distribution in finite size orthotropic plates with blunt notches and holes. *Theoretical and Applied Fracture Mechanics*, 109, 102768. <https://doi.org/10.1016/j.tafmec.2020.102768>
- [27] Meštrović, M. (2020). *Finite element method*. Zagreb, Faculty of Civil Engineering.
- [28] Kalay, O. C., Karaman, H., Karpat, F., Doğan, O., Celallettin Yüce, C., Karpat, E., Dhanasekaran, L., & Khandaker, M. (2021). A Comparative 3D Finite Element Computational Study of Stress Distribution and Stress Transfer in Small-Diameter Conical Dental Implants. *Technical Gazette*, 28(6), 2045-2054. <https://doi.org/10.17559/TV-20200518180158>
- [29] Tuna, M. & Trovalusci, P. (2021). Stress distribution around an elliptic hole in a plate with 'implicit' and 'explicit' non-local models. *Composite Structures*, 256, 113003. <https://doi.org/10.1016/j.compstruct.2020.113003>
- [30] Turnić, D., Marković, N., & Igić, T. (2021). Stress Analysis of Steel Plate Girders Subjected to Patch Loading in Elastoplastic Domain. *Technical Gazette*, 28(4), 1408-1414. <https://doi.org/10.17559/TV-20190416142242>
- [31] ANSYS 5.4, program package

**Contact information:****Mladen RADOJKOVIĆ, prof.**

(Corresponding author)

University of Pristina,

Faculty of Technical Sciences, Kosovska Mitrovica,

Knjaza Milosa 7, 38220 Kosovska Mitrovica, Serbia

E-mail: mladen.radojkovic@pr.ac.rs

**Blaža STOJANOVIĆ, prof.**

University of Kragujevac,

Faculty of Engineering,

Department for Mechanical Constructions and Mechanization,

Kragujevac 34000, Sestre Janjić 6, Serbia

E-mail: blaza@kg.ac.rs

**Saša MILOJEVIĆ, expert advisor.**

University of Kragujevac,

Faculty of Engineering,

Department for Motor Vehicles and Engines,

Kragujevac 34000, Sestre Janjić 6, Serbia

E-mail: sasa.miloevic@kg.ac.rs

**Dejan MARIĆ, PhD.**

(Corresponding author)

University of Slavonski Brod,

Mechanical Engineering Faculty in Slavonski Brod,

Trg Ivane Brlić Mažuranić 2, HR-35000 Slavonski Brod, Croatia

E-mail: dmaric@unisb.hr

**Slobodan SAVIĆ, prof.**

University of Kragujevac,

Faculty of Engineering,

Department for Applied Mechanics and Automatic Control,

Serbia, Kragujevac 34000, Sestre Janjić 6, Serbia

E-mail: ssavic@kg.ac.rs

**Aleksandar SKULIĆ, PhD.**

(Corresponding author)

University of Kragujevac,

Faculty of Engineering,

Department for Mechanical Constructions and Mechanization,

Kragujevac 34000, Sestre Janjić 6, Serbia

E-mail: aleksandarskulic@gmail.com

**Božidar KRSTIĆ, prof.**

University of Kragujevac,

Faculty of Engineering,

Department for Motor Vehicles and Engines,

Serbia, Kragujevac 34000, Sestre Janjić 6, Serbia

E-mail: bkrstic@kg.ac.rs